

Received August 29, 2018, accepted September 21, 2018, date of publication October 1, 2018, date of current version October 25, 2018.

Digital Object Identifier 10.1109/ACCESS.2018.2872753

Energy-Aware Dynamic Resource Allocation in UAV Assisted Mobile Edge Computing Over Social Internet of Vehicles

LONG ZHANG^{ID1}, ZHEN ZHAO¹, QIWU WU², HUI ZHAO¹, HAITAO XU^{ID3}, AND XIAOBO WU⁴

¹School of Information and Electrical Engineering, Hebei University of Engineering, Handan 056038, China

²Department of Armaments Management and Support, Engineering University of PAP, Xi'an 710086, China

³School of Computer and Communication Engineering, University of Science and Technology Beijing, Beijing 100083, China

⁴China Academy of Transportation Sciences, Beijing 100029, China

Corresponding author: Long Zhang (zhanglong@hebeu.edu.cn)

This work was supported in part by the National Natural Science Foundation of China under Grant 61402147, Grant 61802107, and Grant 61501406, in part by the Research Program for Top-notch Young Talents in Higher Education Institutions of Hebei Province, China, under Grant BJ2017037, in part by the Research and Development Program for Science and Technology of Handan, China, under Grant 1621203037, and in part by the Natural Science Foundation of Hebei Province under Grant E2017402115, Grant F2017402068, and Grant F2018402198.

ABSTRACT Social Internet of Vehicles (SIoV) is a new paradigm that enables social relationships among vehicles by integrating vehicle-to-everything communications and social networking properties into the vehicular environment. Through the provision of diverse socially-inspired applications and services, the emergence of SIoV helps to improve the road experience, traffic efficiency, road safety, travel comfort, and entertainment along the roads. However, the computation performance for those applications have been seriously affected by resource-limited on-board units as well as deployment costs and workloads of roadside units. Under such context, an unmanned aerial vehicle (UAV)-assisted mobile edge computing environment over SIoV with a three-layer integrated architecture is adopted in this paper. Within this architecture, we explore the energy-aware dynamic resource allocation problem by taking into account partial computation offloading, social content caching, and radio resource scheduling. Particularly, we develop an optimization framework for total utility maximization by jointly optimizing the transmit power of vehicle and the UAV trajectory. To resolve this problem, an energy-aware dynamic power optimization problem is formulated under the constraint of the evolution law of energy consumption state for each vehicle. By considering two cases, i.e., cooperation and noncooperation among vehicles, we obtain the optimal dynamic power allocation of the vehicle with a fixed UAV trajectory via dynamic programming method. In addition, under the condition of fixed power, a search algorithm is introduced to derive the optimized UAV trajectory based on acceptable ground-UAV distance metric and the optimal offloaded data size of the vehicle. Simulation results are presented to demonstrate the effectiveness of the proposed framework over alternative benchmark schemes.

INDEX TERMS Internet of Vehicles, social networks, unmanned aerial vehicles, mobile edge computing, resource allocation.

I. INTRODUCTION

As a typical mobile Internet of Things, Internet of Vehicles (IoV) has emerged to provide ubiquitous information exchange and content sharing via its internal and external environment with little or no human intervention [1]–[3]. With the help of On-Board Units (OBUs) installed on vehicles and Road-Side Units (RSUs) deployed along the sides of roads, together with benefits of the interaction of vehicle-to-everything techniques, IoV is highly characterized by

gathering, sharing, processing, computing, and secure release of data services onto information platforms [4]. Undoubtedly, IoV has become a promising way to realize the evolution from Intelligent Transportation System into intelligent vehicles [5], autonomous driving [6], electric vehicles [7], and Smart Cities [8]. In addition, the widespread use of smart devices and the recent advances in next generation vehicles promote the inseparable relationships between smart devices and their human carriers. It has become much more possible for drivers

and passengers in IoV scenario to socialize and exchange information with other commuters in the context of temporal-spatial proximity on the roads [1], [9]–[11]. Thus, integration of advanced vehicle-to-everything communications and social networking properties into the IoV environment has emerged as a new paradigm of Social Internet of Vehicles (SIoV) [12], [13].

By enabling social interdependencies among vehicles, SIoV make drivers and passengers enjoy various socially-inspired applications which improve road experience, traffic efficiency, road safety, travel comfort, and entertainment along the roads. For instance, real-time traffic information with drivers' mutual interests, socially-aware interactive navigation, and same trip or route sharing with common preferences are the preferred services. In general, these attractive applications and services that hold massive content volume always require sustainable computation resources and constrained time delays. However, the vehicle-carried OBU often has low computation capability compared to core networks [14], [15]. Due to backhaul loading at peak-hours, it is challenging for core networks to meet the latency requirements of these resource-hungry services. As a result, the tension between resource-limited vehicle-carried terminals and computation-intensive applications becomes the bottleneck for improvement of user satisfaction and quality of experience to socially-aware services in SIoV.

To resolve this issue, mobile edge computing (MEC) has been recognized as a cost-effective method to enhance the computation capability in proximity to mobile devices [16]. It liberates mobile devices from heavy computation workloads, by enabling them to offload computation tasks to nearby MEC servers instead of relying on a remote cloud. Compared with cloud computing, MEC can offer benefits such as low latency by removing long backhaul delay, low energy consumption of mobile devices, and high privacy and security [17], [18]. In this regard, lots of recent efforts and research interests have been attracted from both academia and industry. Especially, SIoV also significantly benefits from MEC applications by deploying high-performance computation and geo-distributed servers at roadside RSUs [14]–[16]. However, rapid mobility of vehicles and radio obstacles due to physical characteristics or external interferences in SIoV make socially-aware service demands of drivers and passengers vary greatly temporally and spatially. To alleviate the workloads at roadside RSUs and reduce the costs of deployed RSUs, unmanned aerial vehicles (UAV) assisted MEC as flying RSUs has been proposed to improve computation performance owing to their low cost and flexible deployment [16]–[20]. Fig. 1 illustrated a typical UAV assisted MEC environment over SIoV under a three-layer integrated architecture, comprising physical-world layer, edge computing layer, and social networking layer. In physical-world layer, the physical objects (e.g., vehicles, smart devices, OBUs, drivers, and passengers) form vehicular networks via vehicle-to-vehicle (V2V) and vehicle-to-infrastructure (V2I) communications. The popular social contents such as traffic and trip

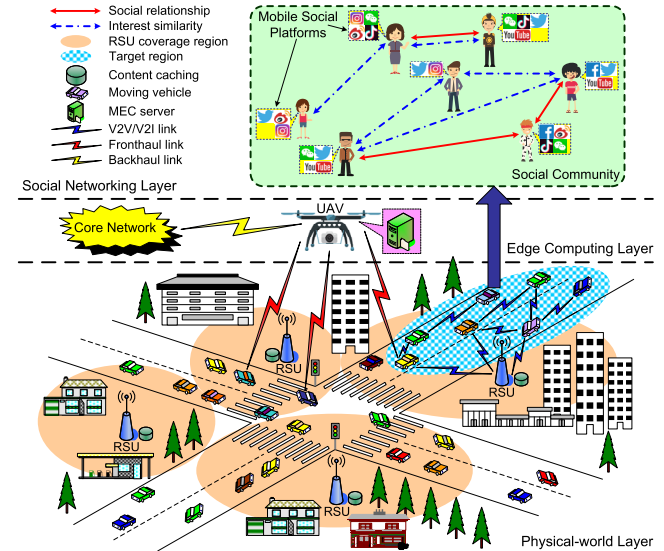


FIGURE 1. Illustration of the UAV assisted MEC environment over SIoV under a three-layer integrated architecture.

sharing information generated by social-based applications and mobile social platforms are cached at roadside RSUs during off-hours, to reduce backhaul loading at peak-hours. In edge computing layer, UAV acting as flying RSUs support the MEC services by executing offloaded computation tasks from vehicles. Finally, the social relationships of vehicles are constructed according to their social ties and interest similarities in social networking layer. Motivated by the above discussions, we can find that the UAV assisted MEC system under the scenario of the SIoV architecture will become highly valuable. Correspondingly, our objective in this paper is to achieve the energy-aware optimal resource allocation by maximizing the total utility under the condition of this architecture. To the best of our knowledge, this is the first work that considers the joint design framework to optimize both the transmit power of vehicle and the UAV trajectory in the UAV assisted MEC environment over SIoV.

A. RELATED WORK

Many works have been dedicated to resource allocation in MEC environment, and most of them were focused on joint computation offloading and resource allocation [21]–[25]. In [21], the total revenue maximization problem was studied by jointly integrating computation offloading decision, resource allocation, and content caching. In [22], the framework of joint computation offloading and interference management was developed from the perspective of MEC computing overhead in terms of execution time and energy. In [23], by leveraging the collaborative properties of augmented reality applications, the resource allocation method for both communication and computation resources was proposed, aiming to reduce sum energy consumption of all users. In comparison with the mentioned optimization objectives in [21]–[23], the work in [24] concentrates on maximizing the weighted sum computation rate by jointly optimizing the

computing mode selection and the system transmission time allocation. In [25], the virtual resource allocation strategy for communication, computing and caching was defined as joint optimization problem, by taking into account the virtualization architecture of information centric heterogeneous networks.

In UAV assisted wireless networks, there also have been some recent studies that focused on either resource allocation or trajectory optimization [26]–[29]. In [26], the power allocation scheme for sum-rate maximization in UAV assisted communication system was presented, which reduces energy consumption for UAV with non-orthogonal multiple access. In [27], the resource allocation problem for UAV assisted networks was investigated, and the average throughput was maximized by satisfying the energy causality constraint under a harvest-transmit-store model. In addition, some other research efforts have been devoted to the issue of joint transmit power and trajectory optimization. In [28], the cooperative throughput maximization problem was studied, which optimizes transmit power, power-splitting ratio and trajectory of UAV in UAV assisted cooperative system with wireless information and power transfer. In [29], the throughput maximization problem in UAV enabled relaying systems was explored by optimizing source/relay transmit power along with UAV relay trajectory.

There are even fewer works for resource allocation in UAV assisted MEC system [19], [20]. In [19], under the mobile cloud computing architecture based on a UAV-mounted cloudlet, the minimization of total energy consumption was investigated by jointly optimizing bit allocation, computation, and trajectory. In [20], the computation rate maximization problem in UAV enabled MEC wireless powered system was studied under both partial and binary computation offloading modes, in which computation resources and transmit power are derived. Most of the works in UAV assisted MEC system were mainly focused on integrated architecture or platform [17], [30], [31] and cyber-threat detection [18].

Although that the theoretical studies has made impressive progress in resource allocation in MEC environment [21]–[25], resource allocation and trajectory optimization in UAV assisted wireless networks [26]–[29], and resource allocation in UAV assisted MEC system [19], [20], our work differs from them based on two points. First, resource allocation and trajectory optimization in their works were to optimize one or several objectives through the assumption that finite time horizon is divided into fixed time slots in a discrete way. However, our work is to conduct dynamic resource allocation in which the transmit power and UAV trajectory should be dynamically adjusted according to the current instant time in the practical dynamic environment. Secondly, their works were primarily targeted at the static network setting involving simple users, sensors, and wireless devices. Those nodes were assumed to be statically located at fixed positions in the networks. However, we study the dynamic resource allocation in UAV assisted MEC environment over dynamic SIoV, wherein

each vehicles belong to the rapidly moving nodes. The mobility properties of vehicles result in the dynamic trajectory of vehicles and the time varying SIoV topology with respect to time dependency. Therefore, the dynamic network topology of SIoV poses extra challenges on optimizing UAV trajectory.

B. MAIN CONTRIBUTIONS

In this paper, our goal is to achieve the energy-aware optimal resource allocation by maximizing the total utility under the UAV assisted MEC environment over SIoV. To reach this goal, we investigate the optimization framework for the total utility maximization problem by jointly allocating the transmit power of vehicle and optimizing the trajectory of UAV. The main contributions of the paper are summarized as follows.

- An approximate approach is designed to generate the probability distribution of the access efficiency associated with a given social content in social content library by leveraging mathematical statistics method. Based on this approximate probability distribution, a popularity factor of a given social content is defined, which determines the probability that the caching server in the RSU stores a part of replicas of the social content.
- We develop a novel optimization framework for the total utility maximization problem by jointly optimizing the transmit power of vehicle and the trajectory of UAV. We convert this optimization problem into an energy-aware dynamic power optimization problem which combines the utility of instant power reduction and the cost of energy consumption for vehicle.
- Under the case of noncooperation and cooperation, we obtain the optimal dynamic power allocation of vehicle with the fixed UAV trajectory by the aid of dynamic programming method. We also rigorously characterize the evolution law of the optimal energy consumption state of vehicle. Besides, with the fixed optimal transmit power, a search algorithm to find the optimized UAV trajectory is presented bearing in mind the acceptable ground-UAV distance metric over the horizontal plane and the optimal data size of the offloaded bits by vehicle.

The remainder of this paper is organized as follows. Section II introduces the system model including the computation and social content caching models, and further presents the problem formulation. In Section III, we propose the framework of the energy-aware dynamic resource allocation, consisting of the transmit power optimization with fixed trajectory and trajectory optimization with fixed power. Simulation results are provided in Section VI, followed by conclusion in Section V.

II. SYSTEM MODEL AND PROBLEM FORMULATION

Consider a UAV assisted MEC system over a SIoV scenario as shown in Fig. 2, where a flying rotary wing UAV is deployed to provide MEC services for a set of $\mathcal{M} = \{1, 2, \dots, M\}$ of M vehicles on the ground within a finite time horizon T . All the vehicles are independent of each other,

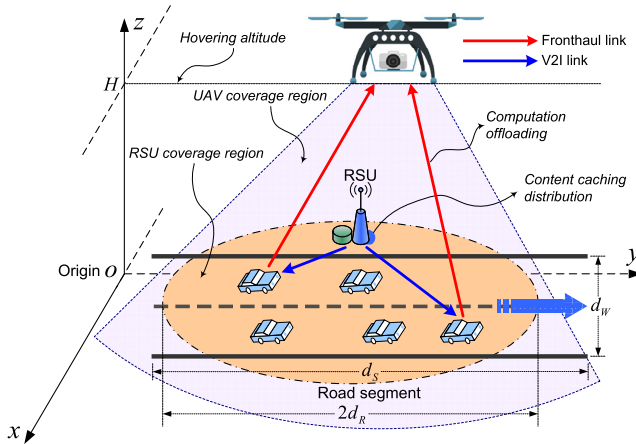
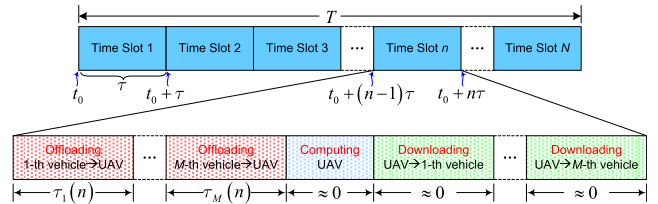


FIGURE 2. The system model.

and are distributed as Poisson point process on the straight unidirectional multi-lane road segment with length d_S and width d_W . We assume that each vehicle drives in a straight line at a constant speed denoted by V , and never leaves the road. The UAV is mounted with a transceiver, a single antenna, and a MEC server. In particular, the MEC server connects to the core network through wireless backhaul and provides computation resources to vehicles by adopting a powerful computing processor. A RSU is installed along the road to make drivers and passengers enjoy the socially-inspired services and require the cached popular social contents via the social content caching server. The cacheable RSU with a radius $d_R \leq d_S/2$ is stationary after deployment. We assume that M vehicles are within the coverage region of the RSU. Thereby, M vehicles can request the cached social contents from the RSU via V2I link. Each vehicle is equipped with a single-antenna OBU which can communicate with the UAV, the RSU and other vehicles. Here, the vehicle-carried OBU has an on-chip microprocessor with limited computing capability to execute local computation task. In this context, the computation task of each vehicle can be partitioned in bitwise for partial local computing and partial computation offloading.

Without loss of generality, we consider a three dimensional Cartesian coordinate system to describe the locations of the ground vehicles and the flying UAV. As shown in Fig. 3, the finite time horizon T is divided into N time slots with equal length τ , i.e., $\tau = T/N$. Let t_n correspond to the instant time within the n th time slot, for $t_n \in [t_0 + (n - 1)\tau, t_0 + n\tau]$, where t_0 is an initial time of time horizon T . It is should be noted that there exist continuous time during each time slot, which differs from fixed time slot division in a discrete way. At the n th time slot, the instant location of the m th vehicle over the horizontal plane coordinate can be denoted as $\mathbf{q}_m(t_n) = [x_m(t_n), y_m(t_n)]$. Under such circumstances, the mobility constraint of the m th vehicle is determined as

$$\|\mathbf{q}_m(T) - \mathbf{q}_m(0)\| = VT \leq 2d_R, \quad \forall m \quad (1)$$

FIGURE 3. The time slot allocation for computation offloading from M vehicles to UAV by using a TDMA-based co-channel media access.

In this system, we focus on the scenario where the UAV flies at a fixed hovering altitude H aiming to keep continuous flying over the air. This stable hovering of the UAV contributes to avoidance of frequent aircraft ascending and descending owing to terrain or building blockage. Then the instant location of the UAV mapped onto the horizontal plane coordinate at the n th time slot can be denoted by $\mathbf{q}_U(t_n) = [x_U(t_n), y_U(t_n)]$. We further assume that the start and end locations of the UAV are pre-determined, which can be also given as $\mathbf{q}_U^s = [x_U^s, y_U^s]$ and $\mathbf{q}_U^e = [x_U^e, y_U^e]$, respectively. Technically, τ can be chosen to be sufficiently small such that the location of the UAV stays approximately at a fixed location at each time slot [20], [28], [32]. In this way, by incorporating the locations of N time slots, the flying trajectory of the UAV within time horizon T can be modeled by $\mathbf{q}_U = \{\mathbf{q}_U^s, \mathbf{q}_U(t_1), \dots, \mathbf{q}_U(t_N), \mathbf{q}_U^e\}$. Thereby, the trajectory constraints of the UAV can be represented as

$$\begin{aligned} \|\mathbf{q}_U(t_n) - \mathbf{q}_U(t_{n-1})\| &\leq \tau V_U^{\max}, \quad \forall n \\ \mathbf{q}_U^s &= \mathbf{q}_U(0), \quad \forall n \\ \mathbf{q}_U^e &= \mathbf{q}_U(T), \quad \forall n \end{aligned} \quad (2)$$

where V_U^{\max} is the UAV's maximum flight speed. We assume that the wireless channel from ground vehicles to the UAV is dominated by the line-of-sight (LoS) transmission link [20], [28], [32]. A quasi-static block fading channel model is utilized to represent the ground-UAV LoS link. In this case, the channel remains unchanged within each fading block, and is subject to distance dependent power attenuation. Therefore, at the n th time slot, the channel gain between the m th vehicle and the UAV can be formulated as

$$h_m(t_n) = \eta_0 d_m^{-\zeta}(t_n) = \frac{\eta_0}{(\|\mathbf{q}_U(t_n) - \mathbf{q}_m(t_n)\|^2 + H^2)^{\zeta/2}} \quad (3)$$

where η_0 is the channel gain at a reference distance d_0 , $d_m(t_n)$ is the distance between the m th vehicle and the UAV over the horizontal plane, and $\zeta \geq 2$ is the path-loss exponent.

A. COMPUTATION MODEL

In this paper, we assume that the vehicles adopt a partial computation offloading model. That is, the computation task can either be executed locally at the vehicles, or be offloaded to and executed by the UAV assisted MEC server. Here, we use the size of computation input data including the program codes and input parameters to describe the computation task

of each vehicle. Let $B_m^{\text{COM}}(t_n)$ (in bits) be the total data size of the computation task for the m th vehicle at the n th time slot. It is clear that $B_m^{\text{COM}}(t_n)$ can be partitioned into two parts, namely, the data size with $B_m^{(L)}(t_n)$ (in bits) executed by the local CPU of the m th vehicle, and the data size with $B_m^{(O)}(t_n)$ (in bits) computed by the UAV.

1) LOCAL COMPUTING

As for a target time slot, we assume that the local computation data for each vehicle must be executed within the corresponding time slot. Let $f_m^{(L)}(t_n)$ (in CPU cycles per second) denote the local computational capability of the m th vehicle at the n th time slot. As such, the total number of CPU cycles required to execute the data size $B_m^{(L)}(t_n)$ is given as $\tau f_m^{(L)}(t_n)$. In addition, we denote the number of CPU cycles required for computing one bit of raw at the m th vehicle as w_m . Thus, the total computation data size executed by local CPU of the m th vehicle at the n th time slot can be calculated by

$$B_m^{(L)}(t_n) = \frac{\tau f_m^{(L)}(t_n)}{w_m} = \frac{T f_m^{(L)}(t_n)}{N w_m} \quad (4)$$

2) COMPUTATION OFFLOADING

In order to avoid the co-channel multiple access interference during computation offloading, we use a TDMA-based media access scheme as exhibited in Fig. 3. To be specific, each time slot is divided into three stages, i.e., the offloading stage, the computing stage, and the downloading stage [20], [33]. In the offloading stage, M vehicles offload their computation data to the UAV one by one during each time slot. For simplicity, we assume that the computation task offloading for M vehicles at each time slot are undertaken on the same frequency band with bandwidth W_C . We represent the transmit power of the m th vehicle at the n th time slot by $p_m(t_n)$. In practice, the instant transmit power $p_m(t_n)$ should be adjusted in a continuous way but must be also limited by the maximum power threshold \bar{P}_m at the n th time slot, i.e., $0 < p_m(t_n) \leq \bar{P}_m$. Thanks to the quasi-static block fading channel model, the maximum power threshold of the m th vehicle at the given ground-UAV distance $d_m(t_n)$ during the n th time slot can be approximately formulated as [34]

$$\bar{P}_m(\text{dBm}) = P_0(\text{dBm}) - 10\zeta \lg \frac{d_m(t_n)}{d_0} \quad (5)$$

$$\bar{P}_m(\text{mW}) = 10^{0.1P_0(\text{dBm}) - \zeta \lg \frac{d_m(t_n)}{d_0}} \quad (6)$$

where P_0 is the receiving reference power by the UAV at a reference distance d_0 . Based on the Shanon-Hartley formula, the achievable transmission rate (in bps/Hz) of the m th vehicle at the n th time slot in the offloading stage can be immediately expressed as

$$\begin{aligned} R_m(t_n) &= \log_2 (1 + \Gamma \cdot \gamma_m(t_n)) \\ &= \log_2 \left(1 + \Gamma \cdot \frac{p_m(t_n) h_m(t_n)}{\sigma^2} \right) \end{aligned} \quad (7)$$

where $\gamma_m(t_n)$ is the achieved signal-to-noise ratio (SNR) along the LoS link from the m th vehicle to the UAV at the n th

time slot, σ^2 is the noise power spectral density at the UAV, and $\Gamma = -\phi_1 / \log_2 (\phi_2 \cdot \text{BER})$ is the constant processing gain factor with ϕ_1 and ϕ_2 depending upon an acceptable bit error rate (BER) of the LoS link along with the specific modulation and coding scheme. We assume a theoretical SNR threshold γ_m^{th} for the m th vehicle to maintain the quality of service (QoS) requirement. Then the achieved SNR of the m th vehicle at the n th time slot should be subject to the QoS constraint, i.e., $\gamma_m(t_n) \geq \gamma_m^{\text{th}}$. Let $E_m(t_n)$ denote the energy consumption state of the m th vehicle at the n th time slot. Similar to [35], the evolution law of the energy consumption state of the m th vehicle can be defined as a linear differential equation as the following

$$\frac{dE_m(t_n)}{dt_n} = \tau \left(p_m(t_n) + \frac{\sigma^2}{h_m(t_n)} \gamma_m(t_n) \right) + E_m(t_n) \quad (8)$$

It is noted that the energy consumption of the m th vehicle is a dynamic variable influenced by the transmit power as well as the achieved SNR and its instant energy consumption level at the n th time slot. Denote by $\tau_m(n)$ the duration allocated to the m th vehicle to offload its computation data to the UAV at the n th time slot. Further considering the communication overhead (e.g., encryption and packer header) denoted by μ_m (in bits) for the m th vehicle during $\tau_m(n)$ [24], the total number of data size to be offloaded to the UAV can be given as $\mu_m B_m^{(O)}(t_n)$, which can be also defined by

$$\mu_m B_m^{(O)}(t_n) = R_m(t_n) \cdot W_C \cdot \tau_m(n) \quad (9)$$

Therefore, the total computation data size of the m th vehicle computed by the UAV at the n th time slot can be written as

$$B_m^{(O)}(t_n) = \frac{W_C \tau_m(n)}{\mu_m} \log_2 (1 + \Gamma \cdot \gamma_m(t_n)) \quad (10)$$

After receiving all the computation data of M vehicles at the n th time slot, the UAV computes and sends the computation results to M vehicles in the downloading stage. In fact, the UAV assisted MEC server has a much powerful computation capability (e.g., a high-speed multi-core CPU) and a much higher transmit power than the ground vehicles [20], [24], [33]. To this end, we can neglect the computing time consumed at the UAV and the downloading time of the vehicle during each time slot as shown in Fig. 3. Thus, the data size with $B_m^{(O)}(t_n)$ of the m th vehicle computed by the UAV at the n th time slot can be rewritten as

$$B_m^{(O)}(t_n) = \frac{W_C \tau}{M \mu_m} \log_2 \left(1 + \Gamma \cdot \frac{p_m(t_n) h_m(t_n)}{\sigma^2} \right) \quad (11)$$

Therefore, under the partial computation offloading model, the total data size $B_m^{\text{COM}}(t_n)$ of the computation task for the m th vehicle at the n th time slot can be written by

$$\begin{aligned} B_m^{\text{COM}}(t_n) &= B_m^{(L)}(t_n) + B_m^{(O)}(t_n) \\ &= \frac{T f_m^{(L)}(t_n)}{N w_m} + \frac{W_C \tau}{M \mu_m} \log_2 \left(1 + \Gamma \cdot \frac{p_m(t_n) h_m(t_n)}{\sigma^2} \right) \end{aligned} \quad (12)$$

Algorithm 1 The Generation Algorithm to Derive Approximate Probability Distribution of the AE of the f th Content

- 1: Initialize the AE of the f th content for M vehicles $\varphi_{f,1}(\Delta T_A), \varphi_{f,2}(\Delta T_A), \dots, \varphi_{f,M}(\Delta T_A)$.
- 2: Sort $\varphi_{f,1}(\Delta T_A), \varphi_{f,2}(\Delta T_A), \dots, \varphi_{f,M}(\Delta T_A)$ in a ascending order with the minimum value labeled by $\varphi'_{f,1}$ and the maximum value labeled by $\varphi'_{f,M}$ to generate a sorted sequence: $\varphi'_{f,1}, \varphi'_{f,2}, \dots, \varphi'_{f,M}$.
- 3: $\forall \varphi_f^{\min}, \varphi_f^{\max} > 0$, for $\varphi_f^{\min} < \varphi'_{f,1}$ and $\varphi_f^{\max} > \varphi'_{f,M}$.
- 4: Divide interval $[\varphi_f^{\min}, \varphi_f^{\max}]$ into L equal subintervals: $\varphi_f^{\min} = \rho_0 < \rho_1 < \rho_2 < \dots < \rho_{L-1} < \rho_L = \varphi_f^{\max}$.
- 5: **for** $\ell = 1 \rightarrow L$ **do**
- 6: $\rho_\ell - \rho_{\ell-1} = (\varphi_f^{\max} - \varphi_f^{\min})/L$.
- 7: Calculate the number of the AE of the f th content within subinterval $(\rho_{\ell-1}, \rho_\ell]$ denoted by Φ_ℓ .
- 8: Calculate the probability value by using $\xi_{f,\ell} = \Phi_\ell/M$.
- 9: **end for**
- 10: **Return** $P(\xi_f) = \{\xi_{f,1}, \xi_{f,2}, \dots, \xi_{f,L}\}$.

B. SOCIAL CONTENT CACHING MODEL

We consider a social content library of F contents, denoted by a set $\mathcal{F} = \{1, 2, \dots, F\}$. The content size of the f th social content is defined as s_f (in bps), for $f \in \mathcal{F}$. We assume that a ground vehicle can be abstracted into a social node, regardless of how many passengers in the vehicle except the driver will access the cached social contents via the RSU. Due to limited caching capacity, the caching server in the RSU can only store a part of replicas of the contents according to the popularity of the social contents. Next, we turn to formulate the popularity of the f th content. For a given time duration $\Delta T_A \gg T$, the access efficiency (AE) of the f th content for the m th vehicle can be defined as the average access duration under one access of the f th content, which is specifically given by

$$\varphi_{f,m}(\Delta T_A) \triangleq \frac{D_{f,m}(\Delta T_A)}{A_{f,m}(\Delta T_A)}, \quad \forall f \in \mathcal{F} \quad (13)$$

where $D_{f,m}(\Delta T_A) > 0$ (in seconds) is the access duration of the f th content under a given ΔT_A , and $A_{f,m}(\Delta T_A) > 0$ is the access numbers of the f th content under a given ΔT_A . Note that the AE $\varphi_{f,m}(\Delta T_A)$ can be considered as a random variable due to the uncertainty of the access duration and the access numbers of the f th content caused by the popularity of social content for the m th vehicle. By using the mathematical statistics method, we propose an approximate approach in Algorithm 1 to generate the probability distribution of the AE of the f th content. We wish to remark that the probability distribution $P(\xi_f)$ follows a complete probability distribution, i.e., $\sum_{\ell=1}^L \xi_{f,\ell} = 1$. For a given $\alpha \in (0, 1]$, the popularity factor of the f th content, denoted by β_f , can be formally formulated as

$$\beta_f \triangleq \sup \{ \theta_f | \Pr \{ \xi_f \geq \theta_f \} \geq \alpha \}, \quad \forall f \in \mathcal{F} \quad (14)$$

where θ_f is the pre-defined random variable. It is worth noting that the higher β_f will result in the case that the f th content

will be more popular for the ground vehicles. Due to the constraint of limited caching capacity, the RSU need to decide whether to cache the replica of the social content via a caching strategy. To describe whether the social content of the f th content has been cached at the RSU, we devise a caching decision profile as a binary matrix given as follows

$$\mathbf{G} = [g_f]_{1 \times F} \quad (15)$$

where g_f is a binary variable, which should satisfy

$$g_f = \begin{cases} 1, & \text{If the } f\text{th content is cached at the RSU} \\ 0, & \text{Otherwise} \end{cases} \quad (16)$$

We use r_m to denote the content request rate of the m th vehicle. According to [36], the content request probability that arises from the m th vehicle can be expressed as

$$\varpi_m = \frac{r_m}{\sum_{m=1}^M r_m} \quad (17)$$

To sum up, the total number of bits of the social content caching distributed by the RSU for the m th vehicle at the n th time slot can be obtained as follows

$$B_m^{\text{CAC}}(t_n) = \sum_{f=1}^F \tau \cdot g_f \cdot \beta_f \cdot s_f \cdot \varpi_m \quad (18)$$

C. PROBLEM FORMULATION

Under the above setup, our objective is to maximize the total utility by jointly combines the computation bits in (12) and the caching bits in (18), while optimizing the transmit power of each vehicle and the trajectory of the UAV. Mathematically, the problem can be formulated as follows.

(P1) :

$$\begin{aligned} \max_{P, \mathbf{q}_U(t_n)} \quad & \sum_{m=1}^M \sum_{n=1}^N \lambda_m \left[\frac{W_C \tau}{M \mu_m} \log_2 \left(1 + \Gamma \cdot \frac{p_m(t_n) h_m(t_n)}{\sigma^2} \right) \right. \\ & \left. + \frac{T f_m^{(L)}(t_n)}{N w_m} + \sum_{f=1}^F \tau g_f \beta_f s_f \varpi_m \right] \end{aligned} \quad (19)$$

$$\begin{aligned} \text{s.t. } C1 : \quad & t_0 + (n-1)\tau \leq t_n \leq t_0 + n\tau, \quad \forall n \\ C2 : \quad & 0 < p_m(t_n) \leq \bar{P}_m, \quad \forall n, \forall m \\ C3 : \quad & \gamma_m(t_n) \geq \gamma_m^{\text{th}}, \quad \forall n, \forall m \\ C4 : \quad & \frac{dE_m(t_n)}{dt_n} = \tau \left(p_m(t_n) + \frac{\sigma^2}{h_m(t_n)} \gamma_m(t_n) \right) \\ & + E_m(t_n), \quad \forall n, \forall m \\ C5 : \quad & \|\mathbf{q}_U(t_n) - \mathbf{q}_U(t_{n-1})\| \leq \tau V_U^{\text{max}}, \\ & \mathbf{q}_U^s = \mathbf{q}_U(0), \quad \mathbf{q}_U^e = \mathbf{q}_U(T), \quad \forall n \\ C6 : \quad & \|\mathbf{q}_m(T) - \mathbf{q}_m(0)\| \leq 2d_R, \quad \forall m \end{aligned} \quad (20)$$

where $\mathbf{P} = [p_m(t_n)]_{N \times M}$ is the transmit power allocation matrix for M ground vehicles within time horizon T , and $\lambda_m > 0$ is the weight of the m th vehicle which characterizes

both the priority and the fairness among all the vehicles. C1 is the instant time constraint within the time horizon. C2 limits the transmit power level of each vehicle for computation offloading. C3 guarantees the QoS requirement for each vehicle. C4 represents the evolution law constraint of energy consumption state for each vehicle. C5 expresses the UAV's trajectory constraint and the start and end location constraint of the UAV, respectively. Finally, C6 specifies the mobility constraint of each vehicle. It is worth noting that the optimization problem (P1) in (19) under the constraints of (20) is evidently non-convex with respect to $\{\mathbf{P}, \mathbf{q}_U(t_n)\}$, which cannot be simply solved with the standard convex optimization techniques. Therefore, it is necessary to transform and simplify the optimization problem (P1) through an appropriate setting of subproblem. In the following, we first investigate the subproblem of the optimization problem (P1), i.e., energy-aware dynamic power optimization with the fixed UAV trajectory. Then, we consider the trajectory optimization under the framework of energy-aware power optimization.

III. ENERGY-AWARE DYNAMIC RESOURCE ALLOCATION

A. PROBLEM TRANSFORMATION

From the optimization problem (P1), we can easily observe that if we allocate the maximum power threshold \bar{P}_m to the m th vehicle with the fixed trajectory of the UAV, the total utility maximization can be easily achieved. However, the total utility maximization is attained at the expense of energy consumption of each vehicle. Obviously, this maximum power allocation is not an optimal solution to the optimization problem (P1). Thus, we are inclined to devise the first subproblem (P2), aiming to derive a trade-off between the optimal power allocation and the energy consumption of each vehicle.

Due to the constraint of the maximum power threshold, the value of power reduction for the m th vehicle at the n th time slot is equal to $\bar{P}_m - p_m(t_n)$. Thus, the efficiency of power reduction for the m th vehicle at the n th time slot can be expressed as

$$\delta_m(t_n) = \frac{\bar{P}_m - p_m(t_n)}{\bar{P}_m} \quad (21)$$

We use $\delta_m(t_n)$ to denote the price factor for power reduction for the m th vehicle at the n th time slot. Therefore, the utility of power reduction for the m th vehicle at the n th time slot can be given as $\delta_m(t_n) \cdot (\bar{P}_m - p_m(t_n))$. Similar to [35], we also denote by ψ the factor to balance the units of the power reduction and the energy consumption. By taking the utility of power reduction and the cost of energy consumption

into account, we then formulate the utility function as follows

$$U_m(t_n) = \frac{\bar{P}_m - p_m(t_n)}{\bar{P}_m} (\bar{P}_m - p_m(t_n)) - \psi E_m(t_n) \quad (22)$$

Our objective is to maximize the utility function in (22) throughout the entire time slot by choosing the optimal transmit power and the optimal energy consumption of each vehicle with the fixed UAV's trajectory. Thus, we convert the total utility maximization problem (P1) into a subproblem (P2) to maximize the utility function in (22) with respect to $p_m(t_n)$ throughout the n th time slot. Specifically, the subproblem can be mathematically formulated as

$$(P2) : \arg \max_{p_m(t_n), m \in \mathcal{M}} \int_{t_0 + (n-1)\tau}^{t_0 + n\tau} e^{-\varepsilon(t_n - t_0 - (n-1)\tau)} \times \left(\frac{(\bar{P}_m - p_m(t_n))^2}{\bar{P}_m} - \psi E_m(t_n) \right) dt_n \quad (23)$$

$$\text{s.t. } C1, C2, C4 \quad (24)$$

where $\varepsilon \in (0, 1)$ is the constant discount factor by which the future utility must be multiplied in order to obtain the present value. The remaining work is thus to solve the subproblem (P2) under the cooperation or noncooperation cases.

B. OPTIMAL POWER ALLOCATION: NONCOOPERATION CASE

The selfish behavior in the partial computation offloading brings about the noncooperation case where all the vehicles compete with each other. Under this case, we then concentrate on the derivation of an optimal solution to the subproblem (P2) by applying Bellman's dynamic programming method [37]. Here, we use $p_m^{NC}(t_n)$ to represent the noncooperative optimal solution to the subproblem (P2). For mathematical tractability, we assume that there exists a continuously differentiable auxiliary function $\Upsilon_m^{NC}(p_m, E_m)$ which is subject to the partial differential equation given by (25) at the bottom of this page.

Theorem 1: The optimal dynamic power allocation $p_m^{NC}(t_n)$ of the m th vehicle constitutes a noncooperative optimal solution to the subproblem (P2) if and only if the optimal power allocation $p_m^{NC}(t_n)$ and the continuously differentiable auxiliary function $\Upsilon_m^{NC}(p_m, E_m)$ are respectively given by

$$p_m^{NC}(t_n) = \bar{P}_m \left(1 - \frac{\tau \psi}{2(1-\varepsilon)} \right) \quad (26)$$

$$\frac{\partial \Upsilon_m^{NC}(p_m, E_m)}{\partial E_m(t_n)} = \frac{\psi}{1-\varepsilon} \quad (27)$$

$$\varepsilon \Upsilon_m^{NC}(p_m, E_m) = \arg \max_{p_m(t_n), m \in \mathcal{M}} \left\{ \frac{(\bar{P}_m - p_m(t_n))^2}{\bar{P}_m} - \psi E_m(t_n) + \frac{\partial \Upsilon_m^{NC}(p_m, E_m)}{\partial E_m(t_n)} (\tau(p_m(t_n) + \frac{\sigma^2}{h_m(t_n)} \gamma_m(t_n)) + E_m(t_n)) \right\} \quad (25)$$

$$\frac{3\tau^2 \bar{P}_m}{4} \left(\frac{\partial \Upsilon_m^{NC}(p_m, E_m)}{\partial E_m(t_n)} \right)^2 - (2\tau \bar{P}_m + E_m(t_n)) \frac{\partial \Upsilon_m^{NC}(p_m, E_m)}{\partial E_m(t_n)} + \varepsilon \Upsilon_m^{NC}(p_m, E_m) = 0 \quad (29)$$

Proof: We first perform the maximization operation of the right hand side of (25) with respect to $p_m(t_n)$. After some necessary mathematical simplifications, we can easily obtain the noncooperative optimal dynamic power allocation $p_m^{NC}(t_n)$ given as

$$p_m^{NC}(t_n) = \bar{P}_m \left(1 - \frac{\tau}{2} \frac{\partial \Upsilon_m^{NC}(p_m, E_m)}{\partial E_m(t_n)} \right) \quad (28)$$

Substituting $p_m^{NC}(t_n)$ in (28) into (25), after some algebraic manipulations, we can easily have a partial differential equation given in (29) at the bottom of the previous page. Upon solving the partial differential equation in (29), we can represent the auxiliary function $\Upsilon_m^{NC}(p_m, E_m)$ as the constraint of partial differential equation which can be expressed as in (27). Substituting the partial differential equation constraint (27) into (28), we finally obtain the optimal power allocation $p_m^{NC}(t_n)$ given as in (26) which constitutes the noncooperative optimal solution to the subproblem (P2). ■

Let $E_m^{NC}(t_n)$ be the optimal energy consumption of the m th vehicle at the n th time slot under the noncooperation case. Based on Theorem 1, the evolution law of the optimal energy consumption state of the m th vehicle can be characterized by

$$\frac{dE_m^{NC}(t_n)}{dt_n} = 2\tau\bar{P}_m \left(1 - \frac{\tau\psi}{2(1-\varepsilon)} \right) + E_m^{NC}(t_n) \quad (30)$$

Note that (30) is a linear differential equation. By solving (30), the optimal energy consumption $E_m^{NC}(t_n)$ follows that

$$\begin{aligned} E_m^{NC}(t_n) &= C_1 e^{t_n} - 2\tau\bar{P}_m \left(1 - \frac{\tau\psi}{2(1-\varepsilon)} \right) \\ &= C_1 e^{t_n} - 2\tau 10^{0.1P_0(\text{dBm}) - \zeta \lg \frac{d_m(t_n)}{d_0} - 3} \\ &\quad \times \left(1 - \frac{\tau\psi}{2(1-\varepsilon)} \right) \end{aligned} \quad (31)$$

where $C_1 > 0$ is a constant number. Therefore, the optimal dynamic transmit power allocation matrix for M vehicles within time horizon T can be expressed as

$$\begin{aligned} \mathbf{P}^{NC} (\text{mW}) \\ = \left[10^{0.1P_0(\text{dBm}) - \zeta \lg \frac{d_m(t_n)}{d_0}} \left(1 - \frac{\tau\psi}{2(1-\varepsilon)} \right) \right]_{N \times M}, \quad \forall n, \forall m \end{aligned} \quad (32)$$

C. OPTIMAL POWER ALLOCATION: COOPERATION CASE

Different from the noncooperation case as stated before, the cooperative behavior will also exist in the partial computation offloading. This results in the cooperation case where all the vehicles form a grand coalition through full cooperation for their common interests. Under this case, our objective is to maximize the sum of the utility functions of all the vehicles throughout the entire time slot while satisfying the evolution law constraint of energy consumption state for each vehicle. Hence, we present a dynamic optimization subproblem (P3) as follows to maximize the sum of the utility functions of all the vehicles

$$(P3) : \arg \max_{p_1(t_n), p_2(t_n), \dots, p_M(t_n)} \sum_{m=1}^M \int_{t_0+(n-1)\tau}^{t_0+n\tau} e^{-\varepsilon(t_n-t_0-(n-1)\tau)} \times \left(\frac{(\bar{P}_m - p_m(t_n))^2}{\bar{P}_m} - \psi E_m(t_n) \right) dt_n \quad (33)$$

$$\text{s.t. } C1, C2, C4 \quad (34)$$

Under the cooperation case, we use $p_m^C(t_n)$ to stand for the cooperative optimal solution to the subproblem (P3). We also assume that there exists a continuously differentiable auxiliary function $\Upsilon_m^C(p_m, E_m)$ which satisfies the partial differential equation given in (35) at the bottom of this page.

Theorem 2: The optimal dynamic power allocation $p_m^C(t_n)$ of the m th vehicle constitutes a cooperative optimal solution to the subproblem (P3) if and only if the optimal power allocation $p_m^C(t_n)$ and the continuously differentiable auxiliary function $\Upsilon_m^C(p_m, E_m)$ are respectively expressed by

$$\begin{aligned} p_m^C(t_n) &= \bar{P}_m \left(1 - \frac{\tau \sum_{m=1}^M \psi}{2(1-\varepsilon)} \right) \\ &= \bar{P}_m \left(1 - \frac{\tau M \psi}{2(1-\varepsilon)} \right) \end{aligned} \quad (36)$$

$$\frac{\partial \Upsilon_m^C(p_m, E_m)}{\partial E_m(t_n)} = \frac{\sum_{m=1}^M \psi}{1-\varepsilon} = \frac{M\psi}{1-\varepsilon} \quad (37)$$

Proof: The proof is similar to Theorem 1. The only difference is that the objective function of the subproblem (P3) is to maximize the sum of the utility functions of all

$$\begin{aligned} \varepsilon \Upsilon_m^C(p_m, E_m) &= \arg \max_{p_1(t_n), p_2(t_n), \dots, p_M(t_n)} \\ &\quad \times \left\{ \sum_{m=1}^M \left(\frac{(\bar{P}_m - p_m(t_n))^2}{\bar{P}_m} - \psi E_m(t_n) \right) + \frac{\partial \Upsilon_m^C(p_m, E_m)}{\partial E_m(t_n)} \left(\tau \left(p_m(t_n) + \frac{\sigma^2}{h_m(t_n)} \gamma_m(t_n) \right) + E_m(t_n) \right) \right\} \end{aligned} \quad (35)$$

$$\begin{aligned} \sum_{m=1}^M \left(\frac{\tau^2 \bar{P}_m}{4} \left(\frac{\partial \Upsilon_m^C(p_m, E_m)}{\partial E_m(t_n)} \right)^2 \right) - \tau^2 \bar{P}_m \left(\frac{\partial \Upsilon_m^C(p_m, E_m)}{\partial E_m(t_n)} \right)^2 \\ + (2\tau \bar{P}_m + E_m(t_n)) \frac{\partial \Upsilon_m^C(p_m, E_m)}{\partial E_m(t_n)} - \varepsilon \Upsilon_m^C(p_m, E_m) - \psi \sum_{m=1}^M E_m(t_n) = 0 \end{aligned} \quad (39)$$

the vehicles. We also perform the maximization operation of the right hand side of (35) with respect to $p_m(t_n)$. After some mathematical simplifications, the cooperative optimal dynamic power allocation $p_m^C(t_n)$ can be expressed as

$$p_m^C(t_n) = \bar{P}_m \left(1 - \frac{\tau}{2} \frac{\partial \Upsilon_m^C(p_m, E_m)}{\partial E_m(t_n)} \right) \quad (38)$$

Upon plugging $p_m^C(t_n)$ in (38) into (35), we can also easily obtain a partial differential equation given in (39) at the bottom of the previous page. Next, we turn to derive the derivative of $\Upsilon_m^C(p_m, E_m)$ with respect to $E_m(t_n)$ in (39). Upon solving the partial differential equation, after some simplifications, the auxiliary function $\Upsilon_m^C(p_m, E_m)$ can be written by (37). Then, substituting $\Upsilon_m^C(p_m, E_m)$ in (37) into (38), we obtain the final result in (36), thus completing the proof. ■

Let $E_m^C(t_n)$ be the optimal energy consumption of the m th vehicle at the n th time slot under the cooperation case. By the aid of Theorem 2, it is readily checked that the evolution law of the optimal energy consumption state of the m th vehicle can be given as follows

$$\frac{dE_m^C(t_n)}{dt_n} = 2\tau\bar{P}_m \left(1 - \frac{\tau \sum_{m=1}^M \psi}{2(1-\varepsilon)} \right) + E_m^C(t_n) \quad (40)$$

By solving linear differential equation in (40), the optimal energy consumption $E_m^C(t_n)$ can be obtained as

$$\begin{aligned} E_m^C(t_n) &= C_2 e^{t_n} - 2\tau\bar{P}_m \left(1 - \frac{\tau \sum_{m=1}^M \psi}{2(1-\varepsilon)} \right) \\ &= C_2 e^{t_n} - 2\tau 10^{0.1P_0(\text{dBm}) - \zeta \lg \frac{d_m(t_n)}{d_0} - 3} \left(1 - \frac{\tau \sum_{m=1}^M \psi}{2(1-\varepsilon)} \right) \end{aligned} \quad (41)$$

where $C_2 > 0$ is a constant number. Therefore, the optimal dynamic transmit power allocation matrix for M vehicles within time horizon T can be formulated as

$$\mathbf{P}^C \text{ (mW)} = \left[10^{0.1P_0(\text{dBm}) - \zeta \lg \frac{d_m(t_n)}{d_0}} \left(1 - \frac{\tau M \psi}{2(1-\varepsilon)} \right) \right]_{N \times M}, \quad \forall n, \forall m \quad (42)$$

D. TRAJECTORY OPTIMIZATION

With the fixed power of each vehicle, the subproblem of the optimization problem (P1) to optimize the UAV's trajectory

can be transformed as follows

(P4) :

$$\begin{aligned} \max_{\mathbf{q}_{U(t_n)}} \sum_{m=1}^M \sum_{n=1}^N \lambda_m &\left[\frac{W_C \tau}{M \mu_m} \log_2 \left(1 + \Gamma \cdot \frac{p_m^*(t_n) h_m(t_n)}{\sigma^2} \right) \right. \\ &\left. + \frac{T f_m^{(L)}(t_n)}{N w_m} + \sum_{f=1}^F \tau g_f \beta_f s_f \varpi_m \right] \end{aligned} \quad (43)$$

$$\text{s.t. } C1, C3, C5, C6 \quad (44)$$

where $p_m^*(t_n)$ (W) refers to the given optimal dynamic transmit power of the m th vehicle at the n th time slot under the noncooperation or cooperation case, which can be summarized as

$$p_m^*(t_n) = 10^{0.1P_0(\text{dBm}) - \zeta \lg \frac{d_m(t_n)}{d_0} - 3} \wp^* \quad (45)$$

where \wp^* is an auxiliary variable which is defined as

$$\wp^* = \begin{cases} 1 - \frac{\tau \psi}{2(1-\varepsilon)}, & \text{for noncooperation case} \\ 1 - \frac{\tau M \psi}{2(1-\varepsilon)}, & \text{for cooperation case} \end{cases} \quad (46)$$

Obviously, (43) is a non-convex optimization problem. Thus, we resort to the problem simplification through relaxing some constraints to find a suboptimal solution to subproblem (P4). In what follows, we first characterize an acceptable ground-UAV distance metric over the horizontal plane under the framework of the optimal transmit power. According to the constraint of the theoretical SNR threshold, the achieved SNR of the m th vehicle at the n th time slot should satisfy the QoS constraint $\gamma_m(t_n) \geq \gamma_m^{th}$. This immediately yields that

$$\frac{p_m^*(t_n) h_m(t_n)}{\sigma^2} \geq \gamma_m^{th} \quad (47)$$

Theorem 3: The optimal dynamic ground-UAV distance $d_m^*(t_n)$ for the m th vehicle at the n th time slot must satisfy the following upper bound

$$d_m^*(t_n) \leq \sqrt{\left(\frac{10^{0.1P_0(\text{dBm}) - 3 + \zeta \lg d_0} \eta_0 \wp^*}{\sigma^2 \gamma_m^{th}} \right)^{\frac{1}{\zeta}}} \quad (48)$$

Proof: See Appendix. ■

Note that the upper bound in (48) gives the constraint metric for the trajectory of the UAV over the horizontal plane under the given spatial location of each vehicle. From the subproblem (P4), under the constraint of fixed power, we need to improve the achieved SNR of each vehicle along the LoS link in order to gain the total utility maximization. It is worthy to mention that the achieved SNR of each vehicle along the LoS link can be significantly enhanced by shortening the ground-UAV distance over the horizontal plane. However, under the constraint of the QoS constraint as well as the spatial location of each vehicle, it will not be realistic to arrange

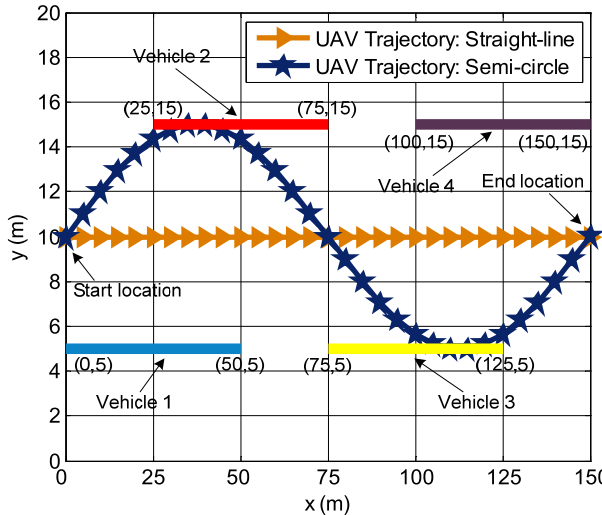


FIGURE 4. Simulation scenario: Two pre-determined benchmark trajectories of UAV and $M=4$ vehicles over the horizontal plane with $N=30$ time slots, unidirectional two-lane road segment with length $d_s = 150\text{m}$ and width $d_W = 20\text{m}$. The straight solid lines marked by vehicle 1, vehicle 2, vehicle 3, and vehicle 4 correspond to the trajectories of $M=4$ vehicles driving from left to right.

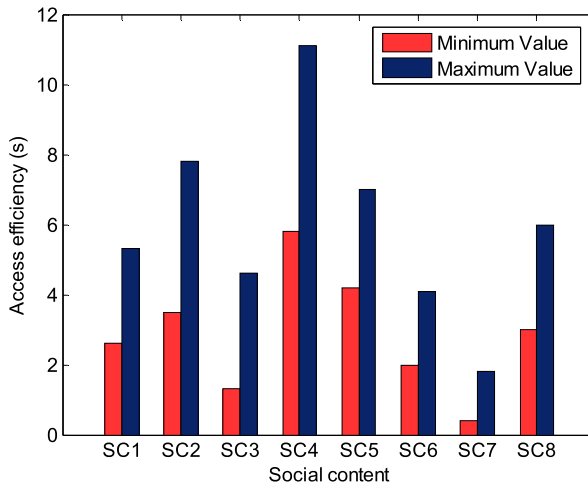


FIGURE 5. Comparison between minimum values and maximum values of AE used in Algorithm 1 among $F=8$ social contents, marked from SC1 to SC8.

an optimal achieved SNR allocation by simply decreasing the ground-UAV distance. After rechecking (43), the total utility maximization depends on how to maximize the total data size computed by the UAV via computation offloading. In order to maximize the total data size of the offloaded bits, each vehicle wants to find out a minimum ground-UAV distance under the condition of single UAV. For a given single UAV, we assume that the minimum ground-UAV distance for the m th vehicle at the n th time slot is denoted by $\tilde{d}_m(t_n) = \sqrt{\|\tilde{\mathbf{q}}_U(t_n) - \tilde{\mathbf{q}}_m(t_n)\|^2 + H^2}$. In theory, for the given $p_m^*(t_n)$ and $\tilde{d}_m(t_n)$, the optimal data size of the m th vehicle computed by the UAV at the n th time slot can be

Algorithm 2 Search Algorithm for Trajectory Optimization

```

1: Initialize  $\zeta, \kappa, A, d_0, \xi, \eta_0, \wp^*, \sigma^2, P_0, \tilde{B}_m^{(O)}(t_n)$ 
2: for  $n = 1 \rightarrow N$  do
3:   for  $m = 1 \rightarrow M$  do
4:     Initialize  $\mathbf{q}_U^{l-1}(t_n), \mathbf{q}_m(t_n)$ .
5:     Calculate  $d_m^{l-1}(t_n) = \sqrt{\|\mathbf{q}_U^{l-1}(t_n) - \mathbf{q}_m(t_n)\|^2 + H^2}$ .
6:     if  $d_m^{l-1}(t_n) \leq \sqrt{(10^{0.1P_0(\text{dBm})-3+\zeta \lg d_0} \eta_0 \wp^*) / (\sigma^2 \gamma_m^{th})}^{\frac{1}{\zeta}}$  then
7:       Set  $l = 1, I_{l-1} = 0, J_{l-1} = \tilde{B}_m^{(O)}(t_n)$ .
8:       Set  $\Xi_1 = 0, \Xi_2 = (\sqrt{5} - 1)/2$ .
9:       Repeat
10:      Set  $I_l = I_{l-1} + \Xi_1(J_{l-1} - I_{l-1}), J_l = I_{l-1} + \Xi_2(J_{l-1} - I_{l-1})$ .
11:      Calculate  $b(J_l)$ .
12:      Update  $B_m^{(O),l}(t_n) = \frac{2b(J_l)}{\pi} B_m^{(O),l-1}(t_n)$  and  $\mathbf{q}_U^l(t_n)$ .
13:      Set  $l = l + 1$ .
14:      Until  $|\tilde{B}_m^{(O)}(t_n) - B_m^{(O),l}(t_n)| < \kappa$ 
15:      Return  $d_m^*(t_n)$  and  $\mathbf{q}_U^*(t_n)$ 
16:    else
17:      go to step 4.
18:    end if
19:  end for
20: end for

```

given as

$$\begin{aligned}
\tilde{B}_m^{(O)}(t_n) &= \frac{W_C \tau}{M \mu_m} \log_2 \left(1 + \Gamma \cdot \frac{\eta_0 p_m^*(t_n) \tilde{d}_m^{-\zeta}(t_n)}{\sigma^2} \right) \\
&= \frac{W_C \tau}{M \mu_m} \log_2 \left(1 + \frac{10^{0.1P_0(\text{dBm})-3+\zeta \lg d_0} \Gamma \eta_0 \wp^*}{\sigma^2} \right. \\
&\quad \times \left. (10^{\lg \tilde{d}_m(t_n)} \tilde{d}_m(t_n))^{-\zeta} \right) \\
&= \frac{W_C \tau}{M \mu_m} \log_2 \left(1 + \frac{10^{0.1P_0(\text{dBm})-3+\zeta \lg d_0} \Gamma \eta_0 \wp^*}{\sigma^2} \right. \\
&\quad \times \left. (\tilde{d}_m^2(t_n))^{-\zeta} \right) \\
&= \frac{W_C \tau}{M \mu_m} \log_2 \left(1 + \frac{10^{0.1P_0(\text{dBm})-3+\zeta \lg d_0} \Gamma \eta_0 \wp^*}{\sigma^2 (\|\tilde{\mathbf{q}}_U(t_n) - \tilde{\mathbf{q}}_m(t_n)\|^2 + H^2)^{\zeta}} \right)
\end{aligned} \tag{49}$$

Based on the optimal data size of the m th vehicle in (49), we next begin by deriving a suboptimal data size of the offloaded bits. In order to obtain the suboptimal data size, we then define a transition function as the searching function. Specifically, for a given transition function $b : \mathbb{R}^+ \rightarrow \mathbb{R}^+$ on a domain $x \in \mathbb{R}^+$, the transition function can be calculated as

$$b(x) = \arctan \left(\frac{x}{A} \right) \tag{50}$$

where $A > 0$ corresponds to an adjusting scalar. It is noted that $b(x)$ is a monotonically increasing function with a trend of more and more stable growth when $x \rightarrow +\infty$. The reason for adopting $b(x)$ as the transition function is two folds. On one hand, $b(x)$ that follows a rapid descent when $x \leq 5$ helps to adjust the data size of the offloaded bits quickly.

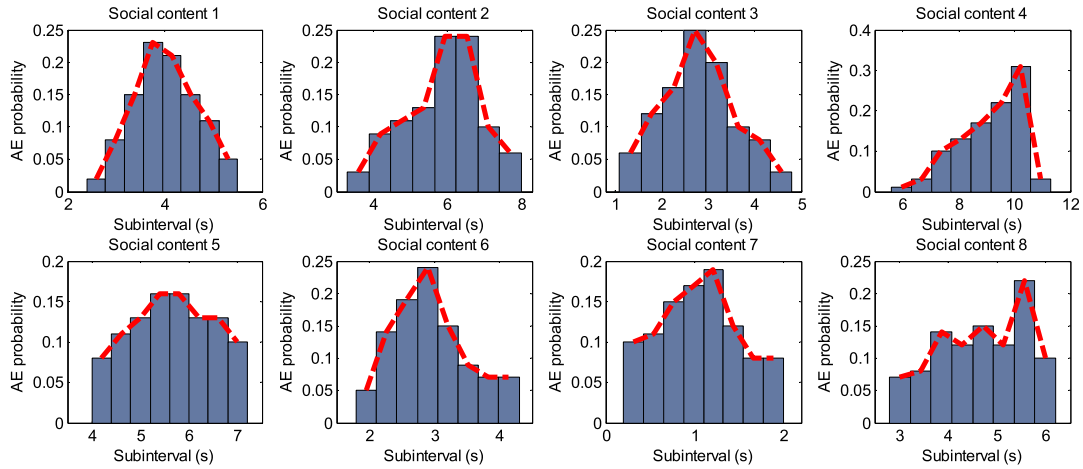


FIGURE 6. Approximate probability distributions of AE generated by Algorithm 1 with the number of subintervals $L=8$ among $F=8$ social contents, marked social content 1 to social content 8, under the constraint of minimum values and maximum values of AE given in Fig. 5.

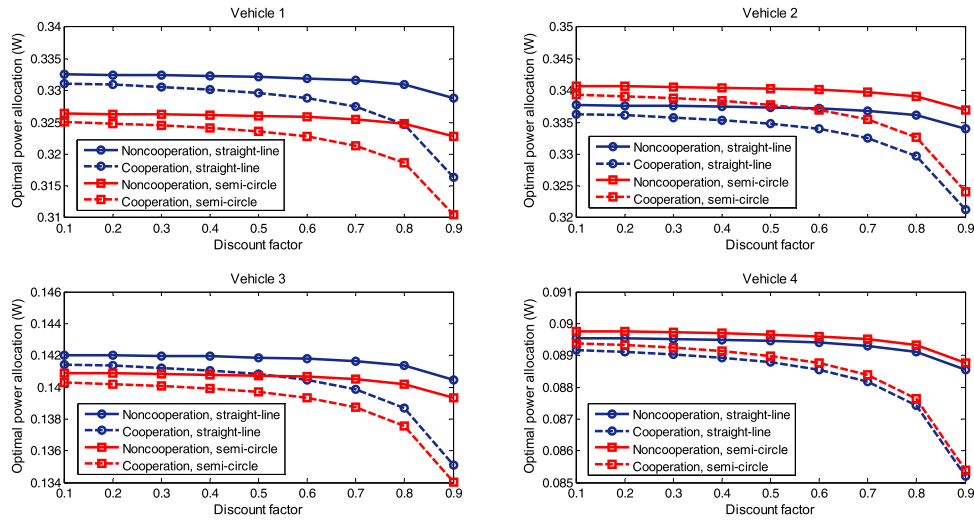


FIGURE 7. Optimal transmit power vs. discount factor among $M=4$ vehicles during 5th time slot with length $\tau = 0.05s$ and UAV hovering altitude $H=50m$.

On the other hand, $b(x)$ is upper bounded by a constant 0.5π , which will aid in controlling the iterations for searching the suboptimal solution. Denote by $\mathbf{q}_U^l(t_n) = [x_U^l(t_n), y_U^l(t_n)]$ the location of the UAV at the l th iteration mapped onto the horizontal plane coordinate at the n th time slot. Similarly, we use $B_m^{(O),l}(t_n)$ to represent the data size of the m th vehicle computed by the UAV at the l th iteration during the n th time slot. Let ς and κ be a search factor and an acceptable tolerant error, respectively, for $\kappa > 0$. Finally, under the given optimal power, we present a search algorithm as summarized in Algorithm 2 for finding a optimized trajectory $\mathbf{q}_U^*(t_n)$ of the UAV.

IV. SIMULATION RESULTS

In this section, we conduct simulations to verify our analysis and evaluate the performance of our proposed framework. As illustrated in Fig. 4, all the simulations are carried

out on a SIoV scenario within a given rectangular area of $20m \times 150m$ over the horizontal plane coordinate. In this scenario, $M=4$ vehicles drive at a same constant speed along a unidirectional two-lane road segment with length $d_S=150m$ and width $d_W=20m$. The start locations and end locations of these vehicles marked by vehicle 1, vehicle 2, vehicle 3, and vehicle 4 are initialized as $(0,5)m$, $(25,15)m$, $(75,5)m$, $(100,15)m$, and $(50,5)m$, $(75,15)m$, $(125,5)m$, $(150,15)m$, respectively. For the benchmark, we consider the case that the UAV flies at a fixed hovering altitude $H=50m$ along two pre-determined trajectories, i.e., straight-line and semi-circle trajectories, with the same start location and end location over the horizontal plane, denoted by $(0,10)m$ and $(150,10)m$. The finite time horizon T is divided into $N=30$ time slots with equal length $\tau = 0.05s$, and the initial time of time horizon T is set to $t_0 = 0s$. We adopt a quasi-static block fading channel model to describe the ground-UAV LoS link.

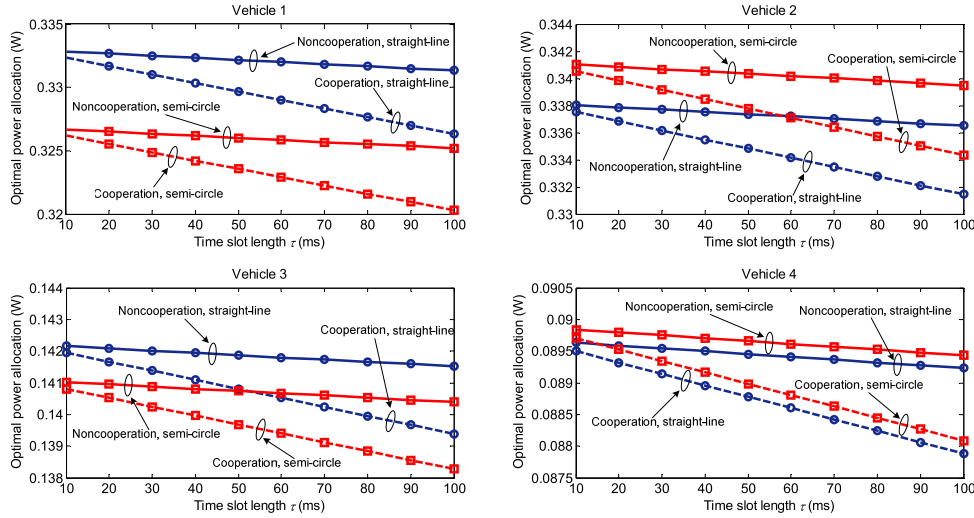


FIGURE 8. Optimal transmit power vs. time slot length among $M=4$ vehicles during 5th time slot with discount factor $\varepsilon = 0.5$ and UAV hovering altitude $H=50m$.

In this model, the path-loss exponent is set to $\zeta = 2$, and the channel gain η_0 at the reference distance $d_0 = 3m$ is assumed to be 9.7×10^{-4} . Moreover, we set the receiving reference power by the UAV at the reference distance $d_0 = 3m$ as $P_0 = 20\text{dBm}$. We further employ a processing gain factor $\Gamma = -1.5 / \log_2(5 \cdot \text{BER})$ where the acceptable BER 10^{-3} of the LoS link for multiple quadrature amplitude modulation with symbol period $52.5\mu\text{s}$. In addition, the noise power spectral density at the UAV is set to $\sigma^2 = -30\text{dBm}$. For the computation model, we assume that each vehicle has the same local computational capability during time horizon T . Then we set the local computational capability $f_m^{(L)}(t_n)$ as 10^6 CPU cycles per second for each vehicle. The number of CPU cycles required for computing one bit of raw at each vehicle is assumed to be $w_m = 5.3 \times 10^{-3}$.

In all the simulations, we consider a social content library of $F=8$ contents which are assumed to have the same content size $s_f=4.6\text{Kbps}$. Due to the lack of empirical data about the AE of social content, we assume that minimum value and maximum value of the AE used in Algorithm 1 among $F=8$ social contents is initialized in Fig. 5. We also set the number of subintervals in Algorithm 1 to $L=8$ for each social content. Under this setting, the approximate probability distribution of the AE generated by Algorithm 1 for $F=8$ social contents can be assumed to satisfy the distribution provided by Fig. 6. The list of other simulation parameters and their values used in this paper are summarized in Table 1.

First the optimal transmit power with the fixed benchmark UAV trajectories with hovering altitude $H=50m$ is compared among $M=4$ vehicles under the cases of noncooperation and cooperation with the continuous evolution of discount factor ε , as depicted in Fig. 7. It is shown that an increased discount factor from 0.1 to 0.9 will reduce the optimal transmit power among $M=4$ vehicles under the noncooperation case or the cooperation case. This is due to the fact that

TABLE 1. System parameters and their values.

Parameter	Value
Acceptable tolerant error κ	0.8
Adjusting scalar in transition function A	2
Balancing factor for the units ψ	0.05
Bandwidth of frequency band W_C	5MHz
Caching decision profile g_f	[1,0,1,1,1,0,0]
Communication overhead μ_m	2000bits
Constant number C_1	10
Constant number C_2	3
Coverage radius of RSU d_R	75m
Content request probability ϖ_m	0.25
Given probability value α	0.1
Pre-defined random variable θ_f	2.8s
Search factor ς	0.3
Theoretical SNR threshold γ_m^{th}	8dB
Weight value for total utility λ_m	[0.2,0.4,0.1,0.3]

the discount factor has a direct affect on the optimal transmit power of vehicles according to (26) and (36). Specifically, the optimal transmit power of each vehicle is inversely related to discount factor ε regardless of the noncooperation case or the cooperation case. From Fig. 7, it is also clearly revealed that the optimal transmit power of vehicles under cooperation case is obviously lower than that of the noncooperation case. This can be explained by the fact that the maximized sum of the utility functions of all the vehicles under the cooperation case has a bearing on the optimal power allocation in (36) by adding a variable M which varies inversely as the optimal power. This result from Fig. 7 further validates that two benchmark trajectories also impact the optimal transmit power of vehicles due to the time varying ground-UAV distance.

In Fig. 8, we show the optimal transmit power comparison according to the evolution of the time slot length τ from 10ms to 100ms during 5th time slot under the noncooperation and cooperation cases with given discount factor $\varepsilon = 0.5$ and the hovering altitude $H=50m$. It can be immediately observed that the optimal power of vehicles for both the noncooperation and cooperation cases will decrease with the growth of the time slot length τ . This is because based on (26) and (36), the optimal transmit power for both cases is inversely proportional to the time slot length τ . It is worth noting that this observation emphasizes the importance of selecting the proper time interval of time slot on the optimal transmit power. In addition, we can further find that the optimal transmit power of vehicles under cooperation case is also obviously lower than that of the noncooperation case. This can be explained by the fact that the optimal transmit power of vehicles by using our proposed optimization framework entirely depends on the maximum transmit power \bar{P}_m , time slot length τ , and discount factor ε .

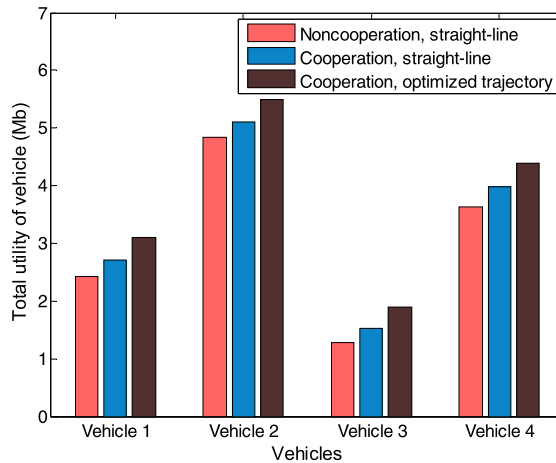


FIGURE 9. Comparison of total utility of vehicle among $M=4$ vehicles between benchmark straight-line and optimized trajectory of UAV during time horizon T with $N=30$ time slots, time slot length $\tau = 0.05s$, and UAV hovering altitude $H=50m$.

Fig. 9 and Fig. 10 display the comparison of total utility of individual vehicle between the benchmark UAV trajectories and the optimized trajectory of UAV during time horizon T with $N=30$ time slots, time slot length $\tau = 0.05s$, and UAV hovering altitude $H=50m$. As can be observed, the total utility of individual vehicle based on the optimized trajectory of UAV during time horizon T outperforms the total utility of individual vehicle using the benchmark trajectories. This is because that our proposed optimization framework can obtain the optimized trajectory of UAV and the optimized ground-UAV distance under the condition of the optimal transmit power of vehicles. However, as for the benchmark UAV trajectories, although the optimal transmit power of vehicles has been employed under the noncooperation or the cooperation case, the time varying ground-UAV distance is not the optimized distance due to the mobility of vehicles. Besides, the total utility of individual vehicle by using straight-line

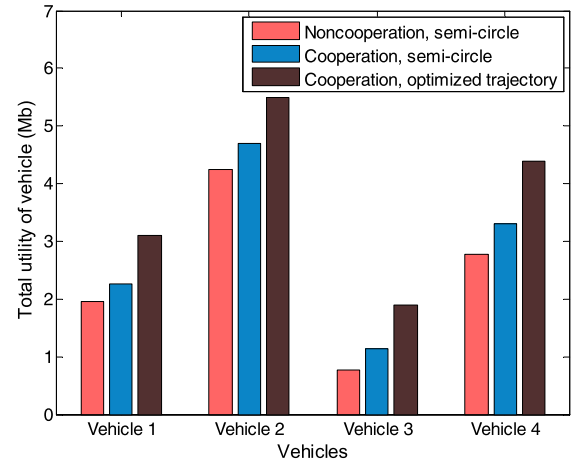


FIGURE 10. Comparison of total utility of vehicle among $M=4$ vehicles between benchmark semi-circle and optimized trajectory of UAV during time horizon T with $N=30$ time slots, time slot length $\tau = 0.05s$, and UAV hovering altitude $H=50m$.

trajectory is more than that of semi-circle trajectory during time horizon T . The explanation is that straight-line trajectory is located in middle positions between trajectories of vehicle 2/vehicle 4 and trajectories of vehicle 1/vehicle 3. Therefore, the time varying ground-UAV distance under straight-line trajectory tends to be an average stable distance in comparison with the complex semi-circle trajectory.

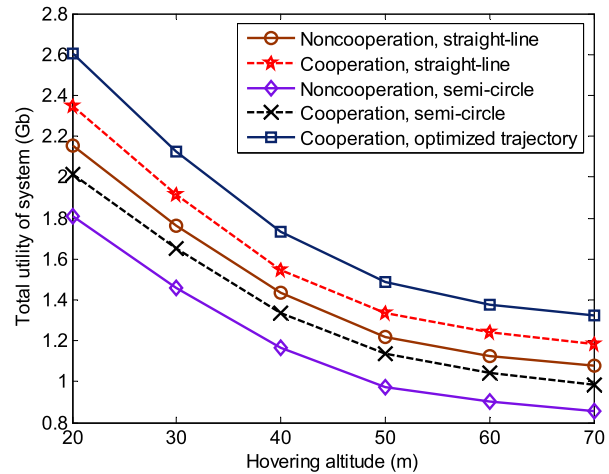


FIGURE 11. Comparison of total utility of system with regard to $M=4$ vehicles for two benchmark trajectories and optimized trajectory of UAV under different UAV hovering altitudes during time horizon T with $N=30$ time slots and time slot length $\tau = 0.05$.

In Fig. 11, we look at the performance of the impact of UAV hovering altitudes H from 20m to 70m on the total utility of system for two benchmark trajectories and the optimized trajectory of UAV during time horizon T with $N=30$ time slots and $\tau = 0.05s$. It can be observed from the figure that the total utility of system decreases with the increase of UAV hovering altitude H from 20m to 70m. On the other hand, the total utility of system based on the optimized trajectory of UAV during time horizon T outperforms the total utility of system using

the benchmark trajectories. This result can be interpreted by the fact that the growth of UAV hovering altitude H will also increase the ground-UAV distance. Apparently, the increased UAV hovering altitude H will reduce the total data size of the offloaded bits by each vehicle. Hence, the total utility of system cannot be maximized in theory. Consequently, lower UAV hovering altitude H yields more total utility of system.

V. CONCLUSION

In this paper, we studied the energy-aware optimal resource allocation problem by maximizing the total utility under the UAV assisted MEC environment over SIoV. We defined the popularity factor of the given social content on the basis of the derived approximate probability distribution of the AE with regard to the given social content. Moreover, we formulated the joint optimization framework of the transmit power of vehicle and the UAV trajectory as the total utility maximization problem. To solve this optimization problem, the energy-aware dynamic power optimization problem was presented, and the optimal dynamic power allocation of vehicle by considering noncooperation and cooperation cases was obtained under the condition of fixed UAV trajectory. Finally, we proposed the search algorithm to find the optimized UAV trajectory with the fixed optimal power according to the acceptable ground-UAV distance metric and the optimal offloaded data size by vehicle, and validated the performance of the proposed framework with simulations. What we have discussed in this paper is the portion of foundation for the optimization framework to achieve the energy-aware resource allocation in the UAV assisted MEC environment over SIoV. In addition, the energy-aware constraint under the proposed framework is formulated bearing in mind the linear differential equation which indicates the evolution law of energy consumption state of vehicle. It is implicitly understood that the usage of this linear differential equation seems to be ideal in currently practical applications of SIoV. Thus, our future work will focus on how to devise and improve the general constraint equation to describe the energy consumption state of vehicle.

APPENDIX

PROOF OF THEOREM 3

Firstly, we consider the noncooperation case. Under this case, by substituting $p_m^*(t_n)$ in (45) and the ground-UAV channel gain $h_m(t_n)$ in (3) into the QoS constraint in (47), we have

$$\frac{10^{0.1P_0(\text{dBm})-\zeta \lg \frac{d_m(t_n)}{d_0}-3} \left(1 - \frac{\tau\psi}{2(1-\varepsilon)}\right) \eta_0 d_m^{-\zeta}(t_n)}{\sigma^2} \geq \gamma_m^{\text{th}} \quad (51)$$

For simplicity, we use the auxiliary variable \wp^* to represent $1 - \tau\psi/2(1 - \varepsilon)$. Thus, we have

$$\begin{aligned} \frac{\sigma^2 \gamma_m^{\text{th}}}{10^{0.1P_0(\text{dBm})-3} \eta_0 \wp^*} &\leq 10^{-\zeta \lg \frac{d_m(t_n)}{d_0}} d_m^{-\zeta}(t_n) \\ &= 10^{-\zeta \lg d_m(t_n)} \times 10^{\zeta \lg d_0} \times d_m^{-\zeta}(t_n) \end{aligned} \quad (52)$$

Rearranging (50), we obtain

$$\begin{aligned} \frac{\sigma^2 \gamma_m^{\text{th}}}{10^{0.1P_0(\text{dBm})-3+\zeta \lg d_0} \eta_0 \wp^*} &\leq 10^{-\zeta \lg d_m(t_n)} \times d_m^{-\zeta}(t_n) \\ &= \left(10^{\zeta \lg d_m(t_n)} d_m(t_n)\right)^{-\zeta} \end{aligned} \quad (53)$$

After taking $10^{\zeta \lg d_m(t_n)} = d_m(t_n)$ into account, we have:

$$\left(d_m^2(t_n)\right)^{\zeta} \leq \frac{10^{0.1P_0(\text{dBm})-3+\zeta \lg d_0} \eta_0 \wp^*}{\sigma^2 \gamma_m^{\text{th}}} \quad (54)$$

As a result, it can readily be shown that

$$\begin{aligned} d_m(t_n) &\leq \sqrt{\left(\frac{10^{0.1P_0(\text{dBm})-3+\zeta \lg d_0} \eta_0 \wp^*}{\sigma^2 \gamma_m^{\text{th}}}\right)^{\frac{1}{\zeta}}} \\ &= \sqrt{\left(\frac{10^{0.1P_0(\text{dBm})-3+\zeta \lg d_0} \eta_0}{\sigma^2 \gamma_m^{\text{th}}} \left(1 - \frac{\tau\psi}{2(1-\varepsilon)}\right)\right)^{\frac{1}{\zeta}}} \end{aligned} \quad (55)$$

Now, the theorem is proved for the noncooperation case that the optimal dynamic ground-UAV distance should satisfy the upper bound constraint as given in (55). Hereinafter, we consider the cooperation case when the auxiliary variable is given by $\wp^* = 1 - \tau M\psi/2(1 - \varepsilon)$. Similar to the proof of upper bound under the noncooperation case, we can repeat the above argument and show that

$$d_m(t_n) \leq \sqrt{\left(\frac{10^{0.1P_0(\text{dBm})-3+\zeta \lg d_0} \eta_0}{\sigma^2 \gamma_m^{\text{th}}} \left(1 - \frac{\tau M\psi}{2(1-\varepsilon)}\right)\right)^{\frac{1}{\zeta}}} \quad (56)$$

To summarize, by combining (55) and (56), we claim that the optimal dynamic ground-UAV distance $d_m^*(t_n)$ must follow the upper bound constraint given in (48), which completes the proof of Theorem 3.

REFERENCES

- [1] A. Rahim *et al.*, "Vehicular social networks: A survey," *Pervasive Mobile Comput.*, vol. 43, pp. 96–113, Jan. 2018.
- [2] Z. Zhou, C. Gao, C. Xu, Y. Zhang, S. Mumtaz, and J. Rodriguez, "Social big-data-based content dissemination in Internet of vehicles," *IEEE Trans. Ind. Informat.*, vol. 14, no. 2, pp. 768–777, Feb. 2018.
- [3] X. Kong, X. Song, F. Xia, H. Guo, J. Wang, and A. Tolba, "LoTAD: Long-term traffic anomaly detection based on crowdsourced bus trajectory data," *World Wide Web*, vol. 21, no. 3, pp. 825–847, 2018.
- [4] N. Lu, N. Cheng, N. Zhang, X. Shen, and J. W. Mark, "Connected vehicles: Solutions and challenges," *IEEE Internet Things J.*, vol. 1, no. 4, pp. 289–299, Aug. 2014.
- [5] R.-H. Zhang, Z.-C. He, H.-W. Wang, F. You, and K.-N. Li, "Study on self-tuning tyre friction control for developing main-servo loop integrated chassis control system," *IEEE Access*, vol. 5, pp. 6649–6660, 2017.
- [6] X. Sun, H. Zhang, W. Meng, R. Zhang, K. Li, and T. Peng, "Primary resonance analysis and vibration suppression for the harmonically excited nonlinear suspension system using a pair of symmetric viscoelastic buffers," *Nonlinear Dyn.*, vol. 94, no. 2, pp. 1243–1265, Oct. 2018.
- [7] H. Xiong, X. Zhu, and R. Zhang, "Energy recovery strategy numerical simulation for dual axle drive pure electric vehicle based on motor loss model and big data calculation," *Complexity*, vol. 2018, Aug. 2018, Art. no. 4071743.
- [8] W. Zhang, Z. Zhang, and H.-C. Chao, "Cooperative fog computing for dealing with big data in the Internet of vehicles: Architecture and hierarchical resource management," *IEEE Commun. Mag.*, vol. 55, no. 12, pp. 60–67, Dec. 2017.

- [9] A. M. Vegni and V. Loscri, "A survey on vehicular social networks," *IEEE Commun. Surveys Tut.*, vol. 17, no. 4, pp. 2397–2419, 4th Quart., 2015.
- [10] Z. Ning, F. Xia, N. Ullah, X. Kong, and X. Hu, "Vehicular social networks: Enabling smart mobility," *IEEE Commun. Mag.*, vol. 55, no. 5, pp. 49–55, May 2017.
- [11] X. J. Kong *et al.*, "Mobility dataset generation for vehicular social networks based on floating car data," *IEEE Trans. Veh. Technol.*, vol. 67, no. 5, pp. 3874–3886, May 2018.
- [12] T. A. Butt, R. Iqbal, S. C. Shah, and T. Umar, "Social Internet of vehicles: Architecture and enabling technologies," *Comput. Electr. Eng.*, vol. 69, pp. 68–84, Jul. 2018.
- [13] K. M. Alam, M. Saini, and A. E. Saddik, "Toward social Internet of vehicles: Concept, architecture, and applications," *IEEE Access*, vol. 3, pp. 343–357, Mar. 2015.
- [14] Q. Yuan, H. Zhou, J. Li, Z. Liu, F. Yang, and X. S. Shen, "Toward efficient content delivery for automated driving services: An edge computing solution," *IEEE Netw.*, vol. 32, no. 1, pp. 80–86, Jan./Feb. 2018.
- [15] K. Zhang, Y. Mao, S. Leng, Y. He, and Y. Zhang, "Mobile-edge computing for vehicular networks: A promising network paradigm with predictive offloading," *IEEE Veh. Technol. Mag.*, vol. 12, no. 2, pp. 36–44, Jun. 2017.
- [16] Y. Mao, C. You, J. Zhang, K. Huang, and K. B. Letaief, "A survey on mobile edge computing: The communication perspective," *IEEE Commun. Surveys Tuts.*, vol. 19, no. 4, pp. 2322–2358, 4th Quart., 2017.
- [17] N. Cheng *et al.*, "Air-ground integrated mobile edge networks: Architecture, challenges, and opportunities," *IEEE Commun. Mag.*, vol. 56, no. 8, pp. 26–32, Aug. 2018.
- [18] S. Garg, A. Singh, S. Batra, N. Kumar, and L. T. Yang, "UAV-empowered edge computing environment for cyber-threat detection in smart vehicles," *IEEE Netw.*, vol. 32, no. 3, pp. 42–51, May/Jun. 2018.
- [19] S. Jeong, O. Simeone, and J. Kang, "Mobile edge computing via a UAV-mounted cloudlet: Optimization of bit allocation and path planning," *IEEE Trans. Veh. Technol.*, vol. 67, no. 3, pp. 2049–2063, Mar. 2018.
- [20] F. Zhou, Y. Wu, R. Q. Hu, and Y. Qian, "Computation rate maximization in UAV-enabled wireless powered mobile-edge computing systems," *IEEE J. Sel. Areas Commun.*, to be published.
- [21] C. Wang, C. Liang, F. R. Yu, Q. Chen, and L. Tang, "Computation offloading and resource allocation in wireless cellular networks with mobile edge computing," *IEEE Trans. Wireless Commun.*, vol. 16, no. 8, pp. 4924–4938, Aug. 2017.
- [22] C. Wang, F. R. Yu, C. Liang, Q. Chen, and L. Tang, "Joint computation offloading and interference management in wireless cellular networks with mobile edge computing," *IEEE Trans. Veh. Technol.*, vol. 66, no. 8, pp. 7432–7445, Aug. 2017.
- [23] A. Al-Shuwaili and O. Simeone, "Energy-efficient resource allocation for mobile edge computing-based augmented reality applications," *IEEE Wireless Commun. Lett.*, vol. 6, no. 3, pp. 398–401, Jun. 2017.
- [24] S. Bi and Y. Zhang, "Computation rate maximization for wireless powered mobile-edge computing with binary computation offloading," *IEEE Trans. Wireless Commun.*, vol. 17, no. 6, pp. 4177–4190, Jun. 2018.
- [25] Y. Zhou, F. R. Yu, J. Chen, and Y. Kuo, "Resource allocation for information-centric virtualized heterogeneous networks with in-network caching and mobile edge computing," *IEEE Trans. Veh. Technol.*, vol. 66, no. 12, pp. 11339–11351, Dec. 2017.
- [26] M. F. Sohail, C. Y. Leow, and S. Won, "Non-orthogonal multiple access for unmanned aerial vehicle assisted communication," *IEEE Access*, vol. 6, pp. 22716–22727, Apr. 2018.
- [27] H. Wang, J. Wang, G. Ding, L. Wang, T. A. Tsiftsis, and P. K. Sharma, "Resource allocation for energy harvesting-powered D2D communication underlaying UAV-assisted networks," *IEEE Trans. Green Commun. Netw.*, vol. 2, no. 1, pp. 14–24, Mar. 2018.
- [28] S. Yin, Y. Zhao, and L. Li, "UAV-assisted cooperative communications with time-sharing SWIPT," in *Proc. IEEE ICC*, Kansas City, MO, USA, May 2018, pp. 1–6.
- [29] Y. Zeng *et al.*, "Throughput maximization for UAV-enabled mobile relaying systems," *IEEE Trans. Commun.*, vol. 64, no. 12, pp. 4983–4996, Dec. 2016.
- [30] Y. Dong, M. Z. Hassan, J. Cheng, M. J. Hossain, and V. C. M. Leung, "An edge computing empowered radio access network with UAV-mounted FSO fronthaul and backhaul: Key challenges and approaches," *IEEE Wireless Commun. Mag.*, vol. 25, no. 3, pp. 154–160, Jun. 2018.
- [31] N. H. Motlagh, M. Bagaa, and T. Taleb, "UAV-based IoT platform: A crowd surveillance use case," *IEEE Commun. Mag.*, vol. 55, no. 2, pp. 128–134, Feb. 2017.
- [32] Y. Zeng and R. Zhang, "Energy-efficient UAV communication with trajectory optimization," *IEEE Trans. Wireless Commun.*, vol. 16, no. 6, pp. 3747–3760, Jun. 2017.
- [33] F. Wang, J. Xu, X. Wang, and S. Cui, "Joint offloading and computing optimization in wireless powered mobile-edge computing systems," *IEEE Trans. Wireless Commun.*, vol. 17, no. 3, pp. 1784–1797, Mar. 2018.
- [34] N. Patwari, A. O. Hero, M. Perkins, N. S. Correal, and R. J. O'Dea, "Relative location estimation in wireless sensor networks," *IEEE Trans. Signal Process.*, vol. 51, no. 8, pp. 2137–2148, Aug. 2003.
- [35] C. Yang, J. Li, P. Semasinghe, E. Hossain, S. M. Perlaza, and Z. Han, "Distributed interference and energy-aware power control for ultra-dense D2D networks: A mean field game," *IEEE Trans. Wireless Commun.*, vol. 16, no. 2, pp. 1205–1217, Feb. 2017.
- [36] Z. Su, Y. Hui, Q. Xu, T. Yang, J. Liu, and Y. Jia, "An edge caching scheme to distribute content in vehicular networks," *IEEE Trans. Veh. Technol.*, vol. 67, no. 6, pp. 5346–5356, Jun. 2018.
- [37] D. W. K. Yeung and L. A. Petrosyan, *Cooperative Stochastic Differential Games*. New York, NY, USA: Springer, 2005.



LONG ZHANG received the B.E. degree in communication engineering from the China University of Geosciences, Wuhan, China, in 2006, and the Ph.D. degree in communication and information systems from the University of Science and Technology Beijing, Beijing, China, in 2012. In 2017, he was a Visiting Scholar with the School of Computing, Tokyo Institute of Technology, Tokyo, Japan. He is currently an Associate Professor with the School of Information and Electrical Engineering, Hebei University of Engineering, Handan, China, and also a visiting Post-Doctoral Fellow with the ECE department, University of Houston, Houston, TX, USA. His research interests include cognitive radio, vehicular networks, UAV assisted wireless networks, AI enabled networks, and radio resource allocation.



ZHEN ZHAO received the B.E. degree in communication engineering from the Qingdao Institute of Technology, Qingdao, China, in 2018. She is currently pursuing the M.S. degree in computer science and technology with the Department of Communication Engineering, School of Information and Electrical Engineering, Hebei University of Engineering, Handan, China. Her current research interests include UAV enabled networks, mobile edge computing, vehicular social networks, and machine learning.



QIWU WU received the B.E. degree in computer science and technology from Hunan Normal University, Changsha, China, in 2005, and the Ph.D. degree in communication and information systems from the University of Science and Technology Beijing, Beijing, China, in 2010. He was a Post-Doctoral Fellow with Engineering University of PAP, Xi'an, China, where he is currently an Associate Professor. His research interests include Internet of Things, secure communications, and optical networks.



HUI ZHAO received the B.E. degree in information and computing science from Shijiazhuang University, Shijiazhuang, China, in 2017. He is currently pursuing the M.S. degree in computer science and technology with the Department of Communication Engineering, School of Information and Electrical Engineering, Hebei University of Engineering, Handan, China. His current research interests include UAV ad hoc networks, resource allocation, physical-layer security, and big data.



HAITAO XU received the B.E. degree in communication engineering from Sun Yat-sen University, Guangzhou, China, in 2007, the M.E. degree in communication system and signal processing from the University of Bristol, U.K., in 2009, and the Ph.D. degree in communication and information systems from the University of Science and Technology Beijing, China, in 2014. He was as a Post-Doctoral Fellow with the University of Science and Technology Beijing, Beijing, China. He is currently an Associate Professor with the University of Science and Technology Beijing, China. He held a Visiting Professor position with the ECE Department, University of Houston, Houston, TX, USA, from 2016 to 2017. His research interests include wireless communication, cognitive radio, game theory, secure communications, and mobile edge computing.



XIAOBO WU received the Ph.D. degree in communication and information systems from the Department of Communication Engineering, School of Computer and Communication Engineering, University of Science and Technology Beijing, Beijing, China, in 2013. He is currently a Senior Engineer at China Academy of Transportation Sciences. His research interests include Internet of Vehicles, transportation informatization, vehicle trajectory optimization, and intelligent transport system.

• • •